Optical Detection of the Superconducting Proximity Effect

L. H. Greene, A. C. Abeyta, I. V. Roshchin and I. K. Robinson

Department of Physics and Materials Research Laboratory
University of Illinois at Urbana-Champaign, Urbana, IL 61801

J. F. Dorsten, T. A. Tanzer and P. W. Bohn

Department of Chemistry and Materials Research Laboratory
University of Illinois at Urbana-Champaign, Urbana, IL 61801

ABSTRACT

We present the first detection of a superconducting proximity effect by optical techniques. Raman scattering on n^+-InAs is performed through very thin, high-quality, superconducting Nb films grown directly on the (100) InAs surface. The 6 to 10 nm thick Nb films exhibit T_c's of 2.5 to 5.5 K, as measured by electronic transport, and are flat to ~0.5 nm, as measured by x-ray reflectivity. As the Nb/InAs structure is cooled below the superconducting transition temperature, the magnitude of the unscreened LO phonon mode, associated with the surface charge accumulation layer in the InAs, is observed to be enhanced by more than 40%. This reversible change is observed only when the Nb is in good electrical contact with the InAs.

Keywords: Superconducting proximity effect, Raman scattering, mesoscopic superconductivity, superconductor-semiconductor interfaces, superconducting thin films, Nb/InAs.

1. INTRODUCTION

The superconducting proximity effect occurs near the interface of a superconductor and normal metal in good electrical contact.[1] It has been described as the leakage of Cooper pairs from the superconductor to the normal metal. The characteristic distances are the superconducting and the normal-metal coherence lengths on the superconducting and normal sides, respectively. Although this effect has been studied for many years, there are still debates over the proper description of this phenomenon.[2,3]

In order to investigate the basic physics of the proximity effect, systems in which the normal metal is replaced by a semiconductor have been studied.[4] The electronic properties of the semiconductor are tunable by adjusting the doping level, which offers great advantages over all-metal junctions. The Fermi velocity, effective mass and carrier concentration, can each be varied over orders of magnitude. Furthermore, the strength of the intrinsic Schottky barrier which forms at the semiconductor interface can be engineered, or as in the case of InAs, avoided completely.[5]

Raman spectroscopy is a powerful probe of near-surface electronic structure of semiconductors.[6-7] It has also been used to probe effects of material processing on interfaces.[8-11] Using visible excitation, this probe examines only the first few tens of nanometers near the surface. In accumulated or depleted semiconductors, the Raman-active vibrational modes are distinctly different due to the difference in the electronic character of the near-surface and bulk regions. Raman scattering from collective excitations also provides information on the carrier concentration[10] and mobility[13-16] of free charge carriers in the semiconductor and the band-bending associated with the interface.[9] Given these advantages, we have for the first time, used Raman scattering to study the effect of superconducting and normal-state Nb films on the near-surface electronic properties of n^+-InAs. Much of this work has been reported by Dorsten et al.[16]

2. BACKGROUND

In earlier work, the crossover from quasiparticle tunneling to Andreev reflection[17] was studied as a function of Schottky barrier thickness in Nb/InGaAs bilayers.[18] An excess conductance detected at low bias was attributed to the existence of a new current-carrying channel at the isolated superconductor /semiconductor interface. Besides the usual mechanisms of quasi-particle tunneling and Andreev scattering at low and high junction transmittances, respectively[19-21], Cooper-pair tunneling from the superconductor to the semiconductor at very high junction transmittances was postulated. This Cooper pair tunneling is related to earlier work in which a weak excess current was observed in the I-V characteristics of superconductor/insulator/superconductor, S/I/S*, tunnel junctions, where S* is a superconductor just above its critical temperature.[22-23] They attributed a weak excess current to a pair-field susceptibility, manifested as a non-equilibrium pair-current across the barrier, and determined a supercurrent was injected into the normal film. The pair-field susceptibility effect, however, is distinct from Cooper pair tunneling in that the excess current observed was smaller, and it only occurred near the T_c of the normal-state electrode. In Cooper-pair tunneling the effect is larger, and a non-superconducting electrode is used.

The excess conductance at low bias in superconductor/semiconductor junctions was later taken as confirmation of the theory of "reflectionless tunneling" at the interface.[24] This is a mesoscopic effect which relies on *single quasiparticle* phase coherence producing a phase-coherent Andreev reflection. In contrast, Cooper-pair tunneling relies on superconducting *pair* phase coherence.[25] Therefore an interesting controversy has arisen.

Although both mechanisms seem to account for the excess conductance in the low to moderate transmission regime, they deviate substantially in the high-transmittance limit. For example, Cooper-pair tunneling should continue to increase as the barrier strength is lowered, whereas the reflectionless tunneling model predicts the excess current will peak and then decrease with increasing transmittance as weak localization effects due to scattering set in. The functional dependencies of the zero-bias conductance on the normal state conductance are also different for the two models. The Cooper-pair tunneling process is based on the Andreev process, which requires two particles; a transmitted electron and a retroreflected hole, so the tunneling rate scales quadratically with the barrier transmittance. In experimental terms, this means that the zero-bias conductance increases with the square of the normal-state conductance. Reflectionless tunneling contrasts this as the coherent Andreev rate, and therefore the corresponding zero-bias conductance, is predicted to increase linearly with the barrier transmittance.

In order to address this controversy, the effect of a superconducting Nb film on the surface electronic structure of InAs using optical spectroscopy has been studied. InAs is used because, instead of a depletion layer or Schottky barrier, it can form an accumulated region at the surface, which is known to be approximately 5 nm in thickness.[26] Furthermore, proximity effects have been detected in superconductor / InAs structures using transport techniques.[27-32] Although details of the formation of the accumulated region are not well understood, Noguchi et al.[33], in studying the effect of surface reconstruction on the accumulation region, determined that the electronic properties of the surface vary with In- and As-stabilized surfaces and thus proposed that the accumulation region is a result of intrinsic donor-like surface states produced by the surface reconstruction. These changes result in band-bending that is the reverse of that typically observed in n-type III-V materials. The Fermi level is pinned in the conduction band near the surface, and electrons are then trapped at the surface of n^+-InAs.

As a result of the charge accumulation, two regions exist near the (100) InAs surface. Separate longitudinal Raman modes, associated with the bulk and charge accumulation regions, are observed. These are, two coupled phonon-plasmon modes, L_- and L_+, primarily associated with the bulk region, and an unscreened LO phonon mode associated with the charge accumulation region. This later mode is allowed because the magnitude of the wave vector of the LO phonon in the accumulated region is larger than the Thomas-Fermi wave vector, leaving the LO phonon unscreened.[26,34-35]

3. EXPERIMENTAL DETAILS

Thin Nb films are grown by dc-magnetron sputter deposition in a UHV-compatible stainless-steel chamber with a base pressure of less than ~$1x10^{-8}$ Torr. Before the Nb deposition, a gentle, *in-situ* Ar^+ etch is performed to remove any oxide layer on the substrate surface. During the etch, an Ar partial pressure of $2x10^{-4}$ Torr is used and the 3 cm diameter ion gun is held at 75 V and 1.0 mA. The Nb films are then grown in an Ar atmosphere of $7x10^{-3}$ Torr with the sputter gun held at a power of 180 Watts. Single-crystal substrates of highly-doped, n^+-InAs ($n=1.2x10^{19}cm^{-3}$, Sn+S-doped), nominally undoped InAs ($n=1.8 \times 10^{16}$ cm^{-3}) and sapphire are used.

The structural quality of the Nb films is remarkably high. Results of x-ray reflectivity measurements performed on beamline X16C at the National Synchrotron Light Source (NSLS) at Brookhaven are shown in Fig. 1. Here, the reflected intensity is plotted as a function of the wave-vector transfer, $q=2k\sin\theta$, where θ is the incident angle of the x-ray beam. The reciprocal of the periodicity of the observed oscillations is proportional to the film thickness and the maximum wave-vector transfer at which oscillations are observed is related to the flatness of the film. These results reveal that the ~10 nm thick Nb films exhibit a surface roughness of 0.3-0.5 nm, or one atomic layer. Under scanning electron microscopy (SEM) at a resolution of 3 nm, these films are featureless.

The superconducting transition temperature, T_c, of the Nb films are measured using a standard four-probe dc resistance technique. As shown in Fig. 2, the bulk T_c of 9.2K is observed for films thicker than 200 nm. For thinner films, a gradual reduction in T_c is observed with decreased film thickness. Below ~40 nm, a dramatic drop in T_c with decreasing thickness occurs. The T_c for each set of samples is measured both prior to and after the Raman experiments and a decrease in T_c of a few tenths of a degree is seen, which is likely due to surface oxidation.

Raman spectra are collected in a near-backscattering geometry. An Ar^+ laser operated at one of several wavelengths is focused on the sample with a cylindrical lens, giving irradiances ranging from 50-270 W/cm^2. The variation in the irradiances arises from the change in power available at different excitation wavelengths and the need to minimize laser-induced heating. All signal calculations are normalized to constant irradiance. A triple grating spectrometer equipped with a charge coupled device (CCD) camera is used to analyze the scattered radiation. The analysis is performed in the $x(y,z)\bar{x}$ configuration where x, y, and z represent the (100), (010), and (001) directions, respectively. In this geometry, the deformation potential and electro-optic contributions to the LO phonon and coupled phonon-plasmon modes, L_- and L_+, are allowed.[36] Measurements are also performed in the $x(y,y)\bar{x}$ configuration where only the LO phonon is allowed. At temperatures near and below T_c, data are taken in an optical cryostat with the Nb/InAs structures immersed in superfluid helium while the temperature is monitored using a Pt-resistance thermometer buried in the copper block holding the sample.

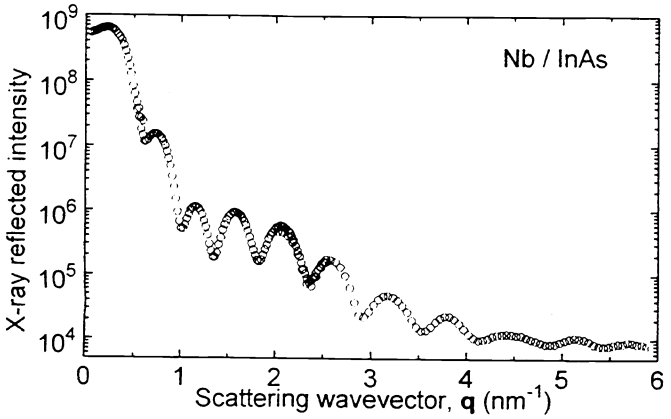

Figure 1: *X-ray reflectivity vs. q-vector for a thin Nb film grown on InAs is shown. The periodicity and number of oscillations indicate the film is about 10 nm thick and smooth to 0.3 - 0.5 nm, respectively.*

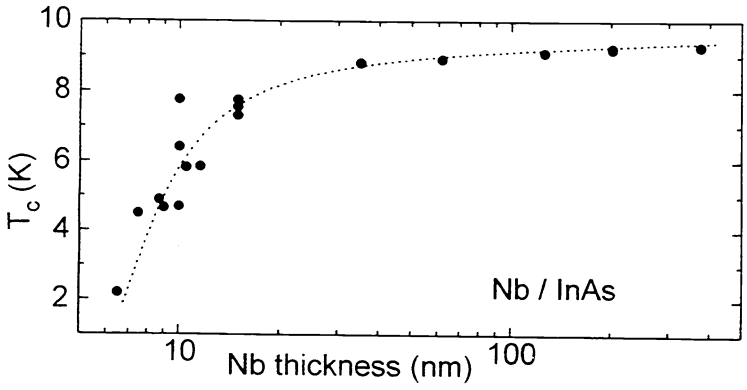

Figure 2: *The T_C vs. Nb film thickness for Nb / InAs structures, grown as described in the text, is shown. The dotted line is a guide for the eye. (After ref. 16)*

4. RESULTS

4.1 Characterization of the InAs surface

The first experiments characterized the InAs before Nb deposition. In order to determine the thickness of the accumulation region and the effects of the InAs surface preparation and deposition of the Nb, Raman spectra were taken on room temperature, bare InAs substrates before and after etching, and on the InAs after Nb deposition. Raman data were also taken on undoped InAs in order to determine the thickness of the accumulated region in the doped InAs. Four excitation wavelengths were used: 488, 514.5, 496.5 and 457.9 nm. The first two wavelengths, 488, 514.5 nm, are at near-resonance with the E_1 gap of InAs at room temperature, and the second two wavelengths, 496.5 and 457.9 nm are at resonance with the E_1 gap at room temperature and 10K, respectively. Results of the Raman data collected at these different wavelengths are presented in Table 1, where the ratio of scattering from the unscreened LO phonon and the L_ collective excitations are shown in relation to the sampling depth.

From the data, it is clear that as the sampling depth increases, the ratio of the LO mode to the coupled mode decreases indicating an increase in scattering from coupled modes which can be seen in the spectra. These results match those reported by Li et al.[35] and support the assertion that the LO mode arises from scattering primarily in the accumulation region while the low-frequency coupled mode is produced from scattering deeper in the bulk. These data, taken with data collected at the same wavelengths on the undoped InAs, can be used to determine the thickness of the accumulation region. These calculations are based on an abrupt junction model in which the width of the accumulation region is determined from[37]: $I^{\lambda}(LO) = I_O^{\lambda}\{1-\exp[-2L_S / d_O(\lambda)]\}$, where I^{λ} and I_o^{λ} are the Raman intensities of the LO phonon from the doped and undoped InAs samples, respectively, L_S is the thickness of the accumulation region, and d_O is the 1/e penetration depth of the excitation beam. Because these calculations are based on measurements taken from two different samples, each Raman intensity measurement consists of an average of at least six measurements taken at different locations to account for surface quality variations and spatial variations in doping. Data from all four excitation wavelengths and different sample locations are used with the abrupt junction model to determine that the width of the charge accumulation region is 3.5 ± 0.3 nm.

TABLE I: Intensity ratios of the LO phonon mode to the coupled phonon-plasmon mode based on sampling depth for several wavelengths.

	Wavelength (nm)	Sampling Depth (nm)	I(LO) / I(L_)
non-resonant	488.0	9.2	0.71
	514.5	13.3	0.58
resonant	457.9	7.5	1.14
	496.5	9.6	0.80

Changes in the interface quality of the n^+-InAs due to the Ar^+ etching are detected by taking Raman spectra of a substrate before and after etching. Earlier Raman studies of damage on $In_xGa_{1-x}As$ surfaces by Ar^+ etching showed lineshapes of the InAs-like and GaAs-like LO phonons were reduced in magnitude and broadened, and at higher damage levels, translational symmetry in the near-surface region was disrupted to the point that disallowed Raman modes (TO) were observed.[8] The Raman spectra of n^+-InAs before and after Ar^+ etching shows that the relative intensity of the LO phonon mode, in comparison to that of the L_ mode, is reduced after etching. This result is seen at room temperature using several wavelengths, and at cryogenic temperatures using 457.9 nm excitation. Raman spectra collected in the $x(y,y)\bar{x}$ geometry, in which the coupled mode is disallowed, show a slight broadening of the LO mode, and the TO mode is not observed. These changes observed in the spectra of our Ar^+-etched InAs single crystal substrates are consistent with some induced disorder in the first few atomic layers of the lattice.

The effects of Nb deposition on the surface of InAs can be studied by measuring the Raman spectra before and after Nb deposition with a set of experiments similar to those reported above. The resulting Raman spectra indicate that Nb deposition causes little change to the etched surface. If the Nb layer is deposited directly on InAs, without etching, only a small decrease in the LO mode intensity is observed. In work reported by Corden et. al[38], deposition of thin metal layers on the (110) surface of n^+-InAs and other III-V semiconductors can cause a change of the relative magnitudes of the LO and TO phonon modes, which is attributed to metal-deposition induced disorder in the interfacial region. A comparison to their work indicates that the Nb deposition in these studies does not drastically damage the InAs surface.

4.2 Temperature-dependent Raman spectroscopy of Nb/InAs structures.

In order to study the effects of normal-state and superconducting Nb on the interfacial electronic structure of InAs, temperature-dependent Raman spectra of Nb / InAs structures taken through the Nb film are compared. As shown in Fig. 3, upon lowering the temperature of the sample below T_c, a dramatic increase in the magnitude of LO phonon scattering is observed, while the magnitude of the L_ coupled mode decreases. Lineshape-fitting calculations reveal that the observed increase in the magnitude of the LO phonon is approximately 40%. This spectral change is reversible upon cycling through T_c.

This reversible enhancement of the LO phonon mode in the Raman spectra is also observed when the surface temperature of the Nb/InAs structure is changed with laser fluence. Holding the structure under superfluid helium and increasing the laser fluence causes the ratio of the peak heights to appear as those in the spectrum taken at 10K. Reducing the laser fluence then returns the spectrum to the appearance it has at 2K.

As a control, the same temperature-dependent Raman spectra are taken on the bare InAs surface. Since the Nb is grown as a strip on the InAs substrate, this only requires moving the laser spot to an uncoated region of the substrate. No detectable change in the intensity ratio of the L_ coupled mode to the LO mode in the spectrum of the bare InAs surface upon cycling between 10 K and 2 K is observed.

The effects of an insulating barrier between the Nb and InAs are investigated by performing the Raman experiments on a sample in which the native oxide on the InAs surface, believed to be at least 3 nm thick, is not removed. For this important control experiment, the Nb is grown on the InAs crystal without an Ar^+ etch. In this case only, the Raman spectra shows no change in peak intensities upon cycling between 2 K and 10 K. We therefore conclude that the reversible effects observed in the temperature-dependent Raman spectra require good electrical contact between the InAs and Nb.

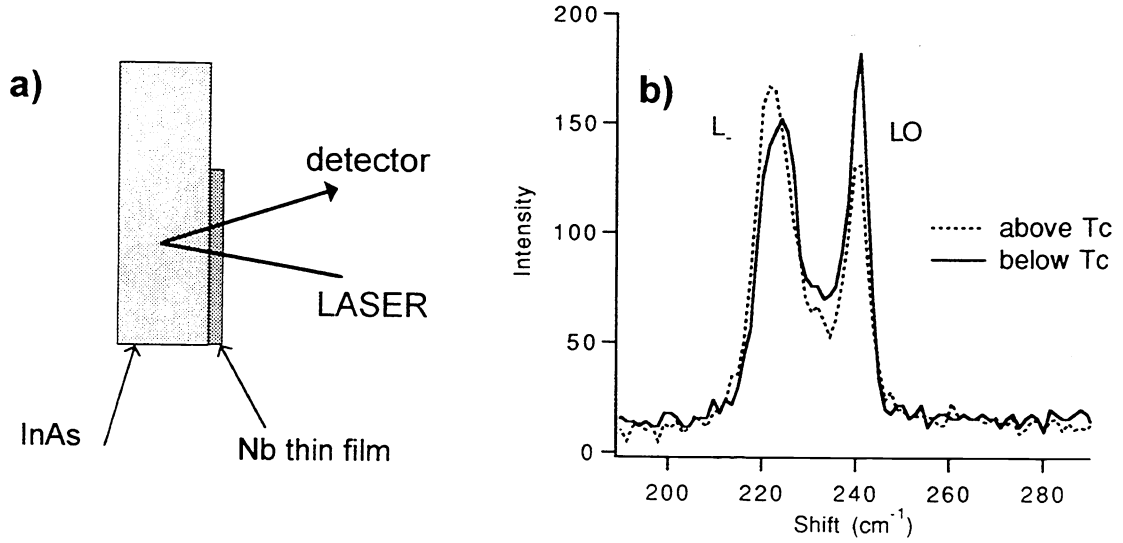

Figure 3. *a) Raman spectra are acquired in a backscatttering geometry through the Nb film as sketched. b) Raman spectra of a Nb/InAs structure above and below T_c are shown by the dotted and full lines, respectively. The low-frequency coupled plasmon-phonon L_ mode is the broad, asymmetric peak about 220 cm^{-1} and the unscreened LO phonon mode is the narrower peak centered at 240 cm^{-1}. As the sample is cooled from 10K to 2K, the relative intensity of the LO mode is increased by ~40%. (After ref. 16).*

5. DISCUSSION

The Raman data are similar to that reported by Ching et. al.[39] who have applied a bias voltage across the (100) surface of p-type InAs and seen a change in the LO phonon intensity relative to the applied field. They attribute this to the change in the effective scattering volume which tracks changes in carrier density. In other work, Buchner and Burstein[30] have placed n^+-InAs in an electrolytic cell and applied electric fields to either deplete or enhance the accumulated surface and saw changes in the low frequency coupled mode intensity which were attributed to changes in free carrier concentration, demonstrating that scattering probes the free carrier concentration in the near-surface region. In both of these works, the applied fields significantly changes both the surface and bulk electronic properties. This is substantially different from our work in which we only observe a subtle change in the coupled phonon-plasmon mode relative to the pronounced change in the LO phonon mode.

The observed changes in the Raman spectrum as the superconducting transition is crossed cannot be due to the superconductivity in the Nb metal alone. First, there is no first-order phase transition in the Nb that would place strain on the InAs, since the experiments are all performed in zero applied magnetic field. Second, any changes in the band-structure properties of the Nb are negligible on the energy scale of the Raman scattering experiment: The Nb superconducting gap in our thin films is less than 1 meV, and would have no effect on the visible probing light nor on the ~29 meV Raman shifts. Finally, the changes in the Raman intensity of the LO mode are only observed when the Nb is in good electrical contact with the InAs.

The increase in LO phonon intensity may be attributed to one or more of the following effects occurring in the surface charge accumulation region: 1) an increase in the scattering volume due to an increase in the width; 2) an increase in the disparity of the electronic properties with the bulk; 3) an increase in the carrier concentration; and 4) a phase correlation of carriers. Each possibility is briefly discussed below.

An increase in the width of the accumulation region would increase the scattering cross-section of the LO phonon with respect to the L_ mode. Since the thickness of the accumulated region is supposedly fixed by the level of doping in the InAs, it is difficult to understand how the width of this region changes upon the T_c crossing. The observation of the LO mode itself is due to the disparity of the electronic properties of the near-surface and bulk regions, and it has been suggested that an increase of this disparity would enhance the LO mode[40]. A proximity effect would certainly increase the conductivity of the region of the InAs juxtaposed with the Nb, but we do not understand how that affects the Raman intensity. If charges were transported from the Nb into the InAs, thereby increasing the carrier concentration as listed in 3) above, the Raman cross-section would necessarily be increased in the InAs and the LO mode would be enhanced. Finally, below the superconducting transition temperature, the electrons and holes in the InAs charge accumulation region must have developed some degree of correlation arising from the Andreev reflection at the interface. Assuming a clean interface and taking into account the differences in the effective masses and Fermi momenta of the two materials, we calculate the ideal probability for Andreev reflection to be 83%. To our knowledge, the effect of a correlated electron plasma on the Raman lattice-mode intensity has not been experimentally or theoretically investigated.

6. CONCLUSION

Changes in the electronic character of the near-surface electronic properties of InAs in intimate electrical contact with superconducting Nb are observed by Raman spectroscopy. The LO phonon mode, associated with the charge accumulation layer at the interface, exhibits a marked increase in relative intensity as compared with the L_ coupled plasmon-phonon mode, primarily associated with the bulk. It is possible that an increase in the carrier concentration in the accumulation layer can account for this effect, but it is also noted that the effect of correlated electrons on Raman cross-section is not known. Therefore, the controversy between Cooper-pair tunneling and reflectionless tunneling has not been settled with the present set of experiments. However, the conclusion that the observed change in the Raman spectra with temperature must be due to a superconducting proximity effect remains. We believe this novel optical method of proximity-effect detection is promising both for studying the basic physics of superconducting interfaces and for possible device applications.

At the high-doping levels of InAs used in these experiments, the mode shift with carrier concentration is negligible in the low-frequency coupled plasmon-phonon mode, L_, studied here. Therefore, in future experiments, we propose to study the high-frequency coupled plasmon-phonon mode, L_+, which is much more sensitive to small changes in the carrier concentration at these high doping levels. Initial experiments show that a shift in the mode frequency can be detected upon deposition of the niobium. Further experiments to study the effects of the superconducting film on the high frequency coupled mode are in progress.

7. ACKNOWLEDGMENTS

The authors are grateful to A. Pinczuk, M. V. Klein, J. Sauls, J. E. Maslar, and G. Blumberg for enlightening conversations on light scattering in inhomogeneous materials, D. Maslov, P. M. Goldbart, D. J. van Harlingen, A. W. Kleinsasser and A. Kastalsky for numerous conversations on superconducting interfaces and P. F. Miceli for discussions on x-ray reflectivity. It is a pleasure to thank W. L. Feldmann for his talented technical assistance.

Authors LHG, ACA, IVR and IKR acknowledge support by the National Science Foundation through the Materials Research Laboratory NSF-DMR-89-20538. Authors JFD, TAT and PWB acknowledge support from the Office of Naval Research N00014-93-1-1168. TAT acknowledges support of the Fannie and John Hertz Foundation. All of the authors are pleased to acknowledge use of the Central Facilities of the Materials Research Laboratory at the University of Illinois, which is supported by the Department of Energy Cooperative agreement through the Materials Research Laboratory under Grant No. DE-FG02-91-ER45439.

8. REFERENCES

1. G. Deutcher, P. G. deGennes in *Superconductivity*, R. D. Parks, ed. (Marcel Dekker, NY, 1969) p1005-1034.
2. Fei Zhou, B. Spivak and A. Zyuzin, Phys. Rev. B **52**, 4467-4472 (1995).
3. I. G A. Devyatov and M. Yu. Kupriyanov, JETP Lett. **59**, 200-205 (1994).
4. For review, see T. M. Klapwijk, Physica B **197**, 481-499 (1994); and A. W. Kleinsasser and W. J. Gallagher in *Superconducting Devices*, D. Rudmann and S. Ruggiero, eds., (Academic Press, Boston, 1989) p325-372,
5. For example, B. G. Streetman, *Solid State Electronic Devices* (Prentice Hall, Englewood Cliffs, NJ, 1990).
6. J. F. Dorsten, J. E. Maslar, and P. W. Bohn, Appl. Phys. Lett. **66**, 1755-1757 (1995).
7. L. A. Farrow, C. J. Sandroff, and M. C. Tamargo, Appl. Phys. Lett **51**, 1931-1933 (1987).
8. J. E. Maslar, J. F. Dorsten, P. W. Bohn, S. Agarwala, I. Adesida, C. Caneau, and R. Bhat, J. Vac. Sci. Tech. B **13**, 988-994 (1995).
9. J. Geurts, Surf. Sci. Rep. **18**, 5-89 (1993).
10. B. Boudart, B. Prevot, and C. Schwab, Appl. Surf. Sci. **50**, 295-299 (1991).
11. P. D. Wang, M. A. Foad, C. M. Sotomayor-Torres, S. Thoms, M. Watt, R. Cheung, C. D. W. Wilkinson, and S. P. Beaumont, J. Appl. Phys. **71**, 3754-3759 (1992).
12. M. Holtz, R. Zallen, O. Brafman, and S. Matteson, Phys. Rev. B **37**, 4609-4617 (1988).
13. A. Mlayah, R. Carles, G. Landa, E. Bedel, and A. Munoz-Yague, J. Appl. Phys. **69**, 4064-4070 (1991).
14. A. Pinczuk, J.M. Worlock, H.L. Stormer, A.C. Gossard, W. Wiegmann, J.Vac. Sci. Tech. **19**, 561-563 (1981).
15. J. S. Kim, D. G. Seiler, and W. F. Tseng, J. Appl. Phys. **73**, 8324-8335 (1993).
16. J. F. Dorsten, T. A. Tanzer, P. W. Bohn, A. C. Abeyta, I. V. Roshchin, and L. H. Greene, submitted to Nature.
17. A. F. Andreev, Sov. Phys JETP **19**, 1228-1231 (1964). [J. Exptl. Theoret. Phys. (U.S.S.R.)].
18. A. Kastalsky, A. W. Kleinsasser, L. H. Greene, R. Bhat, F. P. Milliken, and J. B. Harbison, Phys. Rev. Lett. **67**, 3026-3029 (1991).
19. G. E. Blonder, M. Tinkham, and T. M. Klapwijk, Phys. Rev. B **25**, 4515-4532 (1982).
20. T. M. Klapwijk, G. E. Blonder and M. Tinkham, Physica B+C **109-110**, 1657-1664 (1982).
21. A. W. Kleinsasser, T. N. Jackson, D. McInturff, F. Rammo, G. D. Pettit and J. M. Woodall, Appl. Phys. Lett. **57**, 1811-1813 (1990).
22. F. E. Aspen and A. M. Goldman, J. Low Temp. Phys. **43**, 559-589 (1981).
23. M. Kadin and A. M. Goldman, Phys. Rev. B **25**, 6701-6710 (1982).
24. B. J. van Wees, P. de Vries, P. Magnée, and T. M. Klapwijk, Phys. Rev. Lett. **69**, 510-513 (1992).
25. I. K. Marmorkos, C. W. J. Beenakker, and R. A. Jalabert, Phys. Rev. B **48** 2811-2814 (1993).
26. S. Buchner and E. Burstein, Phys. Rev. Lett. **33**, 908-911 (1974).
27. H. Takayanagi and T. Kawakami, Phys. Rev. Lett. **54**, 2449-2452 (1985).
28. K. Inoue and H. Takayanagi, Phys Rev. B. **43**, 6214-6215 (1991).
29. J. Nitta, T. Akazaki, H. Takayanagi, and K. Arai, Phys. Rev. B **46**, 14,286-14,289 (1992).
30. H. Takayanagi, J. B. Hansen and J. Nitta, Phys. Rev. Lett. **74**, 162-165 (1995).
31. C. Nguyen, J. Werking, H. Kroemer, and E. L. Hu, Appl. Phys. Lett. **57**, 87-89 (1990).
32. C. Nguyen, H. Kroemer, and E. L. Hu, Phys. Rev. Lett. **69**, 2847-2850 (1992).
33. M. Noguchi, K. Hirakawa, and T. Ikoma, Phys. Rev. Lett. **66**, 2243-2246 (1991).
34. C. K. N. Patel and R. E. Slusher, Phys Rev, Lett. **167**, 413-415,(1968).
35. Y. B. Li, I. T. Ferguson, R.A. Stradling, and R. Zaalen, Semicond. Sci. Technol. **7**, 1149-1154 (1992).
36. D. Olego and M. Cardona, Phys. Rev. B **24**, 7217-7232 (1981).
37. H. Shen, F. Pollak, and R. N. Sacks, SPIE Proc. **524**, 145-152 (1985).
38. P. Corden, A. Pinczuk, and E. Burstein, Proc. 10th Intl. Conf. Phys. of Semicond., S. P. Keller, J. C. Hensel, and F. Stern, eds., 739-745 (1970).
39. L. Y. Ching, E. Burstein, S. Buchner, and H. H. Wieder, J. Phys. Soc. Japan **49**, 951-954 (1980).
40. A. Pinczuk, private communication